Author Manuscript

Author Manuscript

Author Manuscript

Author Manuscript

HHS Public Access

Author manuscript

Int J Imaging Syst Technol. Author manuscript; available in PMC 2017 September 19.

Published in final edited form as:

Int J Imaging Syst Technol. 2011 September ; 21(3): 247–252. doi:10.1002/ima.20290.

SPECT Reconstruction with Sub-Sinogram Acquisitions

DoSik Hwang[1], **Jeong-Whan Lee**[2], and **Gengsheng L. Zeng**[3]

[1]School of Electrical and Electronic Engineering, Yonsei University, Seoul, Korea

[2]School of Biomedical Engineering, College of Biomedical and Life Science, Konkuk University, Chung Ju, Korea

[3]Department of Radiology, University of Utah, Salt Lake City, UT, USA

Abstract

Described herein are the advantages of using sub-sinograms for single photon emission computed tomography image reconstruction. A sub-sinogram is a sinogram acquired with an entire data acquisition protocol, but in a fraction of the total acquisition time. A total-sinogram is the summation of all sub-sinograms. Images can be reconstructed from the total-sinogram or from sub-sinograms and then be summed to produce the final image. For a linear reconstruction method such as the filtered backprojection algorithm, there is no advantage of using sub-sinograms. However, for nonlinear methods such as the maximum likelihood (ML) expectation maximization algorithm, the use of sub-sinograms can produce better results. The ML estimator is a random variable, and one ML reconstruction is one realization of the random variable. The ML solution is better obtained via the mean value of the random variable of the ML estimator. Sub-sinograms can provide many realizations of the ML estimator. We show that the use of sub-sinograms can produce better estimations for the ML solution than can the total-sinogram and can also reduce the statistical noise within iteratively reconstructed images.

Keywords

single photon emission computed tomography; positron emission tomography; reconstruction; sub-sinograms; iterative reconstruction

I. INTRODUCTION

There are generally two approaches used in reconstructing images from projection data (i.e., a sinogram for parallel projections) when considering single photon emission computed tomography (SPECT). One is a linear approach, such as the filtered backprojection (FBP) method, and the other is an iterative method, such as the maximum likelihood expectation maximization (ML-EM) (Shepp and Vardi, 1982; Groch and Erwin, 2000; Bruyant, 2002). The FBP methods have been the most widely used algorithms for image reconstruction during the past several decades due to their high efficiency and easy implementation. With

Correspondence to: DoSik Hwang; dosik.hwang@yonsei.ac.kr.

This work was partially presented at a conference of the Society of Nuclear Medicine.

Author Manuscript Author Manuscript Author Manuscript Author Manuscript

the advance of high-speed computer technology, the iterative methods have become very attractive as they can incorporate both statistical and physical models into the reconstruction process, including Poisson noise characteristics and attenuation. For both image reconstruction approaches, statistical noise has been a challenge. The well studied ML-EM algorithms have been found to produce good results in reconstruction from noisy data as they are based on Poisson statistics (Shepp and Vardi, 1982; Unser and Eden, 1988; Liow and Strother, 1991; Barrett et al., 1994; Qi, 2003; Hwang and Zeng, 2006a). Nevertheless, the ML-EM algorithm still suffers from noise, and many attempts have been made to further reduce this statistical noise (Hebert and Leahy, 1989; Green, 1990; Liow and Strother, 1991; Johnson, 1994; Panin et al., 1999; Selivanov et al., 2001; Nuyts, 2002; Nuyts and Fessler, 2003; Hwang and Zeng, 2005). This article shows that the use of sub-sinograms can contribute to the reduction of noise within a reconstructed image.

A sub-sinogram is a sinogram acquired with an entire data acquisition protocol, but with a fraction of the total scanning time (Buvat, 2002), and a total-sinogram is the summation of all of the sub-sinograms. The concept of sub-sinograms has already been introduced as part of several bootstrap approaches, but their main interests were focused on estimating the noise properties of the reconstructed images (Buvat and Riddell, 2001; Buvat, 2002; Dahlbom, 2002; Groiselle and Glick, 2002). This article shows via our proposed method that the noise can be reduced when the final image is obtained by the summation of reconstructions using sub-sinograms.

In fact, the ML estimator itself is a random variable. One ML reconstruction is one realization of the random variable. The ML solution is better obtained using the mean value of the random variable of the ML estimator. The sub-sinogram method can provide many realizations of the ML estimator and can produce a better estimation of the ML solution. In the following sections, we describe the reconstruction methods using sub-sinograms to show their effects on the nonlinear ML-EM reconstruction methods as well as on the linear FBP method (Hwang and Zeng, 2006b).

II. THEORY

The ML estimator is a random variable having a certain distribution around its expected value. As its realization is random, many samples are needed to estimate the expected value, as a more accurate estimation can be obtained with a higher number of samples. One ML reconstruction is one realization of the random variable; therefore, it is likely to produce a poor estimation. A stronger ML solution can be obtained using the mean value of many random realizations of the ML estimator. However, in common practice, only one data realization (i.e., a total-sinogram) is obtained. Therefore, only one realization of the ML image is produced.

In this article, many sub-sinograms are acquired and the corresponding ML images are produced. Each image that is reconstructed from a sub-sinogram is a poor estimate of the ML solution. However, we will show that the final image estimated using the mean values of these images is a better estimation of the ML solution in comparison with an image reconstructed directly from a total-sinogram. Furthermore, more realizations of the ML

Author Manuscript Author Manuscript Author Manuscript Author Manuscript

estimator can be obtained via combinations of sub-sinograms, which will be described in Section IIIB, and a better estimation can be determined using these combinations.

III. METHODS

A. Sub-Sinogram Measurements and Reconstructions

Sub-sinograms can be obtained by measuring an object multiple times, each with a fraction of the total scanning time. Let the total scanning time be divided into N time intervals, then we have N sub-sinograms, P_1, P_2, …, P_N with "sub" meaning that they include only about $1/N$ total counts (Buvat, 2002). Each P_i, $i = 1, 2, \ldots, N$, is a complete low-count data set. A total-sinogram is a summation of all sub-sinograms, $P_T = P_1 + P_2 + \ldots + P_N$. Images reconstructed from sub-sinograms are represented as I_1, I_2, …, I_N and will be called low-count images in the remainder of this article. The final reconstructed image using sub-sinograms, I_S, is obtained by summing all low-count images, i.e., $I_S = I_1 + I_2 + \ldots + I_N$. The image directly reconstructed from a total-sinogram is I_T. If a reconstruction algorithm is linear, then I_T is expected to be the same as I_S, that is, $I_S = I_T$. If a reconstruction algorithm is nonlinear, then I_T is not the same as I_S, that is, $I_S \neq I_T$.

B. Generation of Additional Sub-Sinograms

More sub-sinograms and their corresponding low-count images can be produced via several sub-sinogram combinations. As each view for every sub-sinogram is independent, a new sub-sinogram can be generated using combined individual views from several sub-sinograms; a sub-sinogram is a $B \times V$ matrix, where B and V represent the number of acquisition bins and projection angles, respectively. A new sub-sinogram can be generated by randomly drawing each column v ($v = 1, \ldots, V$) among the N sub-sinograms. For example, a new sub-sinogram can be generated by combining the 1st column of the 2nd sub-sinogram, the 2nd column of the 7th sub-sinogram, the 3rd column of the 5th sub-sinogram, …, and the Vth column of any other sub-sinogram, etc. In this way, N^V new sub-sinograms can be generated, and the corresponding low-count images can be obtained.

We show how our proposed method affects the FBP and ML-EM methods. In simulation studies, sub-sinograms are generated by dividing the count level of the original noiseless projection data by N and then adding Poisson noise corresponding to the $1/N$ count level. All N sub-sinograms obtained are statistically independent from each other, and the total-sinogram is obtained by summing all N sub-sinograms.

IV. COMPUTER SIMULATION STUDIES

A. Data Generation

In the computer simulations, the phantom consisted of one large uniform disk and two small hot lesions, as shown in Figure 1. The large disk was centered at the axis of the detector rotation with a radius of 25 pixels and density of 1. Each of the small lesions had radii of 5 and 7 with a density of 2. The dimension of the image was 64 × 64, and the number of projection angles was 120 over [0, π). The detector bin size was set to half the image pixel size to make the solutions converge at higher iterations in ML-EM (Hwang and Zeng, 2005),

Author Manuscript Author Manuscript Author Manuscript Author Manuscript

and 10 sub-sinograms were generated. Random Poisson noise was added into each of the sub-sinograms corresponding to its count level, which were 1/10 = 0.1 and 2/10 = 0.2, for the large disk and small hot lesions, respectively. The total-sinogram was obtained by summing all 10 sub-sinograms.

B. Sub-Sinogram Method with FBP

Figure 1 shows the original phantom image (a) and the reconstructed images using the conventional FBP method with the total-sinogram (b), FBP with a single sub-sinogram (c), and the sum of the FBP reconstructions with 10 sub-sinograms (d), all within the presence of Poisson noise. As expected from the linear property of FBP, the sub-sinogram method produced the exact same image as did the conventional FBP with a total sinogram, that is, $I_S = I_T$. Hence, there was no benefit in using sub-sinograms for FBP reconstruction.

C. Sub-Sinogram Method with ML-EM

Three images reconstructed with ML-EM from noisy data were compared, as shown in Figure 2. One was a conventional ML-EM reconstruction using the total-sinogram (a), another was the proposed method with 10 sub-sinograms (b), and the last one was the ML-EM reconstruction with additional 1000 sub-sinograms (c) produced by combinations of the 10 sub-sinograms. The generation of additional sub-sinograms was explained in Section IIIB. The number of iterations for all cases was 500. The high number of iterations with the half-bin-size detector (i.e., when the size of the detector bin is half that of the image pixel size) was previously used to ensure that the solutions converged. Note that Hwang and Zeng (2005) showed that the ML-EM solutions converged at the high number of iterations when a half-bin-size detector was used. All three methods were compared via their converged images. Our proposed methods (b and c) produced less noisy images than did method (a). For quantitative analysis, the noise indices, which were defined as a standard deviation divided by its mean over a uniform region of interest (ROI), shown in Figure 2d, were calculated and compared in Figure 3. Both the sub-sinogram and combination methods resulted in lower noise indices for all four ROIs when compared with that of the conventional total-sinogram method. These values show that our proposed methods reduced the statistical noise in the reconstructed images. Additional noise indices were calculated from the postfiltered reconstructed images with a 2D Gaussian convolution kernel as the postfiltering is commonly applied in practice (Nuyts, 2002). Three different Gaussians with σ's of 0.5, 0.7, and 1.0 were applied to the reconstructed images, and the corresponding noise indices were calculated and provided in Table I. In all three cases, our proposed methods resulted in lower noise indices when compared with that of the conventional total-sinogram method. The same experiments were conducted with different noise realizations and different count levels, producing consistent results. However, in the high count experiments, improvements were small in comparison with those in the low-count cases.

V. EXPERIMENTS WITH THE JASZCZAK PHANTOM

A. Experimental Setup

The Jaszczak phantom (i.e., Data Spectrum Corporation, Fig. 4 left) is a cylindrical acrylic phantom with "cold" inserts of rods and spheres and a region of uniform activity. The

Author Manuscript Author Manuscript Author Manuscript Author Manuscript

phantom was filled with 37.2 mCi of Tc-99m and water, and the projection data was acquired using an IRIX SPECT system (a triple-detector camera, Philips Medical Systems) at the University of Utah Hospital. The projection data was acquired in a 64 × 64 matrix (6.9 × 6.9 mm^2 for each element), and each of the 64 views covered 360°. Twenty sub-sinograms, 4.6 min each, were acquired, and a total-sinogram was obtained by summing all 20 sub-sinograms. The dimensions of the reconstructed image were 64 × 64 (6.9 × 6.9 mm^2 for each element). Transverse slices with uniform activity and cold spheres were reconstructed using the ML-EM method with the total-sinogram, the ML-EM with sub-sinograms, and the ML-EM with combinations of the sub-sinograms. No attenuation correction, scatter correction, or detector blurring correction was performed. Figure 5 shows how the reconstructed image changed as low-count images were accumulated in our proposed sub-sinogram method, with each low-count image being reconstructed from each sub-sinogram. The numbers on the top of the images represent the number of low-count images to be summed. The noise indices for the accumulated images were 0.9561, 0.4901, 0.4239, 0.3684, 0.3231, 0.3142, 0.2912, and 0.2612, respectively. The ROI for the calculation of the noise index was the center uniform area, which had a radius of 6 (pixels) and a pixel count of 112.

B. Noise Comparison

The slice with uniform activity was reconstructed for noise comparisons using the conventional ML-EM algorithm with a total-sinogram, the ML-EM with 20 sub-sinograms, and the ML-EM with 1000 combinations of the sub-sinograms. Figure 6 shows three reconstructed images. The sub-sinogram methods (b) and (c) resulted in less noisy images in comparison with the conventional method (a). Noise indices were calculated over the uniform area (ROI), as shown in Figure 6d, and were 0.3218, 0.2313, and 0.2175 for the ML-EM with the total-sinogram, the ML-EM with sub-sinograms, and the ML-EM with combinations of the sub-sinograms, respectively. These values show that our proposed methods reduced the statistical noise in the reconstruction. These results were consistent with the computer simulation studies in which the use of sub-sinograms produced less noisy images. Figure 7 shows the effect of the number of combinations of sub-sinograms on the reconstruction quality. The curve in Figure 7 is the noise index of the combination ML-EM reconstructions as a function of the number of sub-sinogram combinations. The upper and lower horizontal lines represent the noise indices of the ML-EM using the total-sinogram and of the ML-EM using sub-sinograms, respectively. The noise decreased as the number of combinations increased, which shows asymptotic behavior. The noise index became smaller than that of the sub-sinogram method when more than 120 combinations were used, and when there were over 300 combinations, the improvements were small.

Figure 8 shows the reconstructed images of a sphere-containing slice using the ML-EM with a total-sinogram (a), the ML-EM with 20 sub-sinograms (b), and the ML-EM with 1000 combinations of the sub-sinograms (c). Our proposed methods (b and c) produced less noisy images than that of the conventional method (a). The noise indices over the central uniform area were 0.3459, 0.2612, and 0.2362, respectively.

Author Manuscript Author Manuscript Author Manuscript Author Manuscript

VI. DISCUSSIONS AND CONCLUSIONS

We have shown that the use of sub-sinograms can contribute to the reduction of statistical noise in SPECT image reconstruction. Our studies showed that the summation of the low-count images from sub-sinograms produced a less noisy image than does an image reconstructed from a total-sinogram (i.e., the sum of all sub-sinograms). Furthermore, we produced a higher number of projection sets than the number of sub-sinograms by randomly combining several sub-sinograms to generate new sub-sinograms, from which additional low-count images were reconstructed. The resulting low-count images were summed and scaled into the proper intensity levels. In this way, we further reduced the statistical noise in the final image. This method is applicable to the nonlinear iterative reconstruction algorithms, such as the ML-EM method that was used in our studies. Because of its nonlinear property, the sum of all low-count images (i.e., each low-count image is reconstructed from each sub-sinogram) produces a different, less noisy image than that reconstructed directly from a total-sinogram. However, for the linear reconstruction algorithms, such as the FBP, there is no benefit in using sub-sinograms.

The performance of our proposed method may depend on the number of sub-sinograms. The numbers 10 and 20 in our studies were chosen ad hoc as a feasibility study. There would be a maximum number of sub-sinograms, above which the MLEM algorithm may breakdown as there are too little counts in sub-sinograms to produce low-count images. There would be a minimum number of sub-sinograms, below which the contribution of the sub-sinogram methods to noise reduction may become negligible compared with the conventional total-sinogram method. Therefore, the optimum number of sub-sinograms may depend on the total scan time and total count level.

Another approach to reduce the statistical noise is Baysian reconstruction method. In Bayesian methods, a priori probability density function on the image itself is incorporated into the reconstruction procedure to prevent noise amplification during iterations. It has been shown that Bayesian methods can effectively reduce the statistical noise in the reconstructed images (Hebert and Leahy, 1989; Green, 1990; Nuyts, 2002; Nuyts and Fessler, 2003). However, they tend to introduce artificial appearances such as flat zones, staircasing artifacts, discontinuity over smoothly varying regions, etc., and these artifacts are difficult to remove. In contrast to Bayesian methods, our proposed method does not need any prior knowledge on the image. There is no smooth constraint among neighboring pixels, which is usually adopted in Bayesian methods, and therefore, no such artificial appearances were observed in our reconstructed images. However, in cases where such artificial appearances could be neglected, Bayesian methods would be more effective in reducing statistical noise.

The sub-sinogram methods can be incorporated into the modern gamma cameras. In fact, the experimental data in our study was acquired using IRIX SPECT system with a triple-detector camera. The gamma camera rotated faster than usual, and multiple times, producing sub-sinogram datasets. However, the acquisition efficiency would be somewhat lower than the conventional total-sinogram method as the detector should rotate multiple times, which lengthens the total travel trajectory. As an alternative, a modification to the acquisition software would enable an efficient sub-sinogram acquisition mode by dividing the time

Author Manuscript Author Manuscript Author Manuscript Author Manuscript

interval during acquisition for each angle into several subintervals with the number of sub-sinograms and saving the counts for each of the subintervals. In this manner, sub-sinogram datasets could be acquired without sacrificing the acquisition efficiency.

Each sub-sinogram in our proposed method is basically a complete set of sinogram, to which any reconstruction and compensation method can be applied. Therefore, advanced techniques such as collimator response compensation can be applicable to the sub-sinogram method to further reduce noise. If the collimator response compensation can improve the low-count images in sub-sinograms, the sub-sinogram methods may offer overall image improvement with collimator response compensation. How much improvement can be made with collimator response compensation in sub-sinogram methods may need further intensive investigations, which will be covered in future studies.

In addition to the collimator response compensation, a scatter correction with triple-energy window methods may be applicable to the sub-sinogram methods. The triple-energy window method is a preprocessing technique to remove the scattered components from the projection data measured from the central energy window. The scattered components are estimated from the side windows. The scattered components only contain low frequencies and are smooth. The proposed sub-sinogram method is able to use this preprocessing technique to reduce the scattering effect. To control the noise from the very low-count scattered photon measurements, we can use the total sinogram from the side energy windows to estimate the scattering components. If necessary, a low-pass filter can be applied to the estimated scattering components. Because of the fact that the data in the central energy window are statistically independent from the data acquired from the side energy windows, after subtracting the estimated smoothed scattering components, the sub-sinogram projections are still statistically independent from each other, and the advantages of the sub-sinogram still hold.

The disadvantages of our proposed methods are the increased amount of data and the increased computational time for reconstruction. If N sub-sinograms were acquired, then N times the disk space and computational time would be required in comparison with those of the conventional total-sinogram method. If additional sub-sinograms from combinations were used, much more computational time would be necessary. Fortunately, each reconstruction from each sub-sinogram is an independent process. Therefore, efficient parallel processing methods can be applied to each sub-sinogram to reduce the computational time. With the aid of parallel processing and cheap storage disk, the aforementioned disadvantages can be minimized as reducing the noise in the final reconstructed images.

References

Barrett HH, Wilson DW, Tsui BMW. Noise properties of the EM algorithm. I. Theory. Phys Med Biol. 1994; 39:833–846. [PubMed: 15552088]

Bruyant PP. Analytic and iterative reconstruction algorithms in SPECT. J Nucl Med. 2002; 43:1343–1358. [PubMed: 12368373]

Buvat I. A non-parametric bootstrap approach for analyzing the statistical properties of SPECT and PET images. Phys Med Biol. 2002; 47:1761–1775. [PubMed: 12069092]

Author Manuscript Author Manuscript Author Manuscript Author Manuscript

Buvat I, Riddell C. A bootstrap approach for analyzing the statistical properties of SPECT and PET images. Nucl Sci Symp Conf Rec. 2001; 3:1419–1423.

Dahlbom M. Estimation of image noise in PET using the bootstrap method. IEEE Trans Nucl Sci. 2002; 49:2062–2066.

Green PJ. Bayesian reconstructions from emission tomography data using a modified EM algorithm. IEEE Trans Med Imaging. 1990; 9:84–93. [PubMed: 18222753]

Groch MW, Erwin WD. SPECT in the year 2000: Basic principles. J Nucl Med Technol. 2000; 28:233–244. [PubMed: 11142324]

Groiselle CJ, Glick SJ. Using the bootstrap method to evaluate image noise for investigation of axial collimation in hybrid PET. Nucl Sci Symp Conf Rec. 2002; 2:782–785.

Hebert T, Leahy R. A generalized EM algorithm for 3-D Bayesian reconstruction from Poisson data using Gibbs priors. IEEE Trans Med Imaging. 1989; 8:194–202. [PubMed: 18230517]

Hwang D, Zeng GL. Reduction of noise amplification in SPECT using smaller detector bin size. IEEE Trans Nucl Sci. 2005; 52:1417–1427.

Hwang D, Zeng GL. Convergence study of an accelerated ML-EM algorithm using bigger step size. Phys Med Biol. 2006a; 51:237–252. [PubMed: 16394336]

Hwang D, Zeng GL. SPECT Image reconstruction using sub-sinograms. J Nucl Med. 2006b; 47:374 P.

Johnson VE. A note on stopping rules in EM-ML reconstructions of ECT images. IEEE Trans Med Imaging. 1994; 13:569–571. [PubMed: 18218534]

Liow JS, Strother SC. Practical tradeoffs between noise, quantitation, and number of iterations for maximum likelihood-based reconstructions. IEEE Trans Med Imaging. 1991; 10:563–571. [PubMed: 18222862]

Nuyts J. On estimating the variance of smoothed MLEM images. IEEE Trans Nucl Sci. 2002; 49:714–721.

Nuyts J, Fessler JA. A penalized-likelihood image reconstruction method for emission tomography, compared to postsmoothed maximum-likelihood with matched spatial resolution. IEEE Trans Med Imaging. 2003; 22:1042–1052. [PubMed: 12956260]

Panin VY, Zeng GL, Gullberg GT. Total variation regulated EM algorithm. IEEE Trans Nucl Sci. 1999; 46:2202–2210.

Qi J. A unified noise analysis for iterative image estimation. Phys Med Biol. 2003; 48:3505–3519. [PubMed: 14653559]

Selivanov VV, Lapointe D, Bentourkia M, Lecomte R. Cross-validation stopping rule for MLEM reconstruction of dynamic PET series: Effect on image quality and quantitative accuracy. IEEE Trans Nucl Sci. 2001; 48:883–889.

Shepp LA, Vardi Y. Maximum likelihood reconstruction for emission tomography. IEEE Trans Med Imaging. 1982; MI-1:113–122.

Unser M, Eden M. Maximum likelihood estimation of linear signal parameters for Poisson processes. IEEE Trans Acous Speech Signal Proc. 1988; 36:942–945.

Author Manuscript Author Manuscript Author Manuscript Author Manuscript

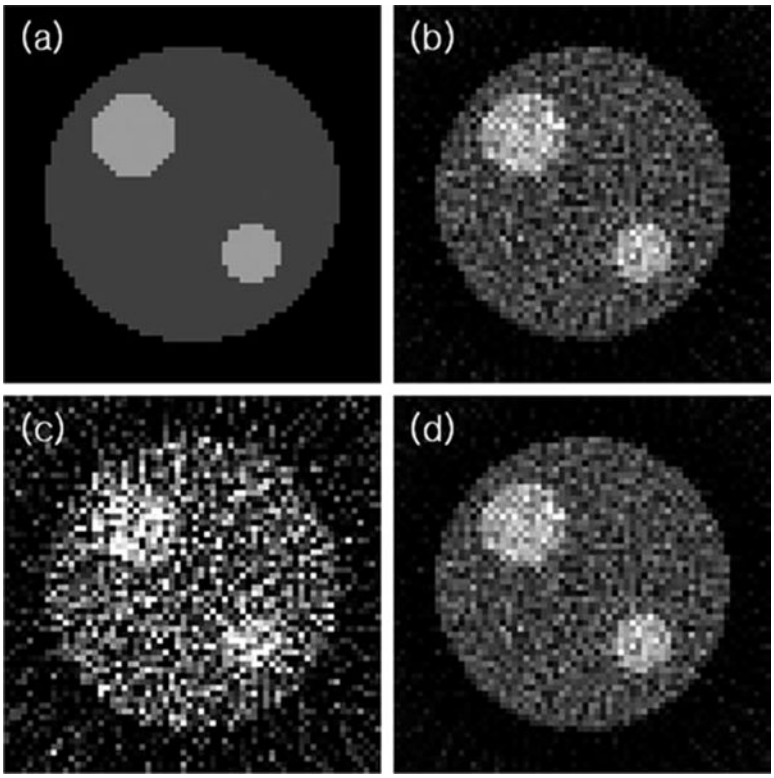

Figure 1.
Sub-sinogram methods with FBP: (a) original image, (b) FBP reconstruction with a total-sinogram, (c) FBP reconstruction with a single sub-sinogram, and (d) sum of FBP reconstructions with 10 sub-sinograms. The images (b and d) are the same, illustrating that there was no benefit in using sub-sinograms with the FBP method.

Author Manuscript Author Manuscript Author Manuscript Author Manuscript

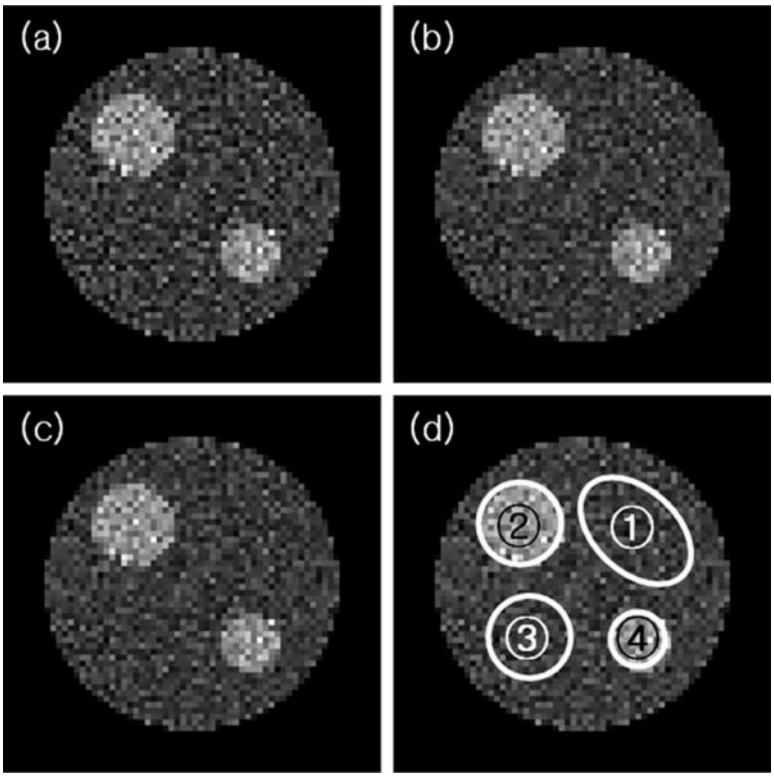

Figure 2.
Sub-sinogram methods with ML-EM: (a) conventional ML-EM with total-sinogram, (b) ML-EM with 10 sub-sinograms, (c) ML-EM with 1000 combinations of the 10 sub-sinograms, and (d) regions of interest (ROI) for noise comparison.

Author Manuscript Author Manuscript Author Manuscript Author Manuscript

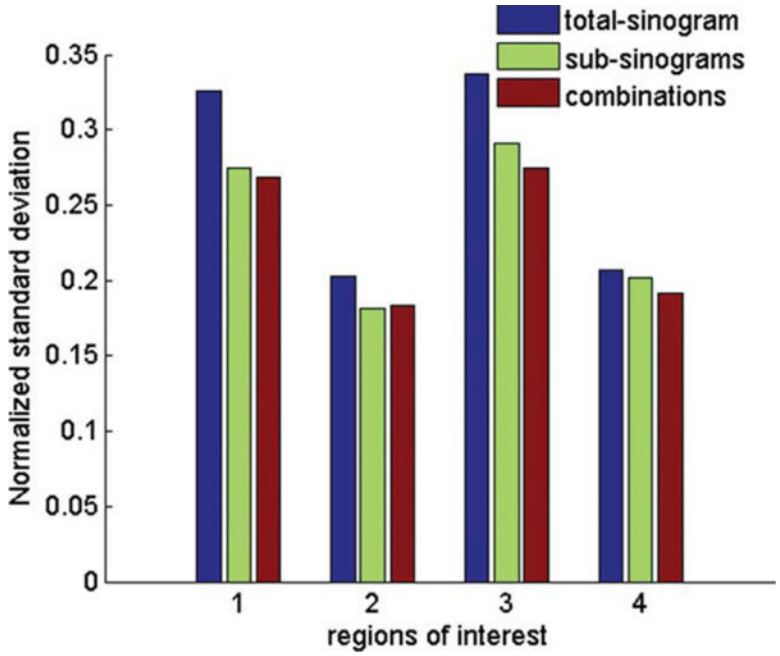

Figure 3.

Noise comparison for four ROIs. Noise indices over four ROIs were calculated. In all ROIs, the sub-sinogram method and combination method produced less noisy results than did the conventional total-sinogram method. In the first, third, and fourth ROIs, further improvements were observed when using the combination method. [Color figure can be viewed in the online issue, which is available at wileyonlinelibrary.com.]

Author Manuscript Author Manuscript Author Manuscript Author Manuscript

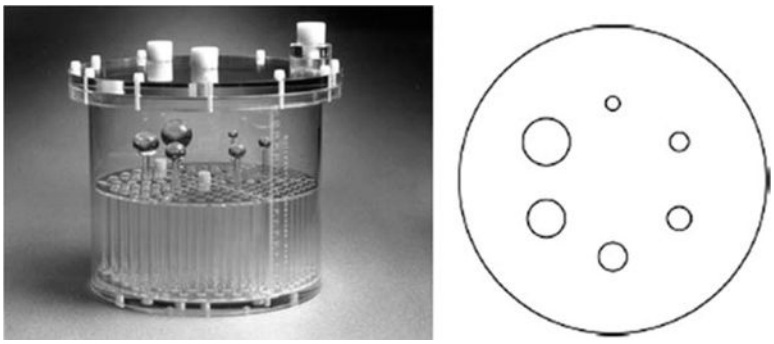

Figure 4.
A Jaszczak phantom (left), and a transverse slice with cold spheres (right).

Author Manuscript Author Manuscript Author Manuscript Author Manuscript

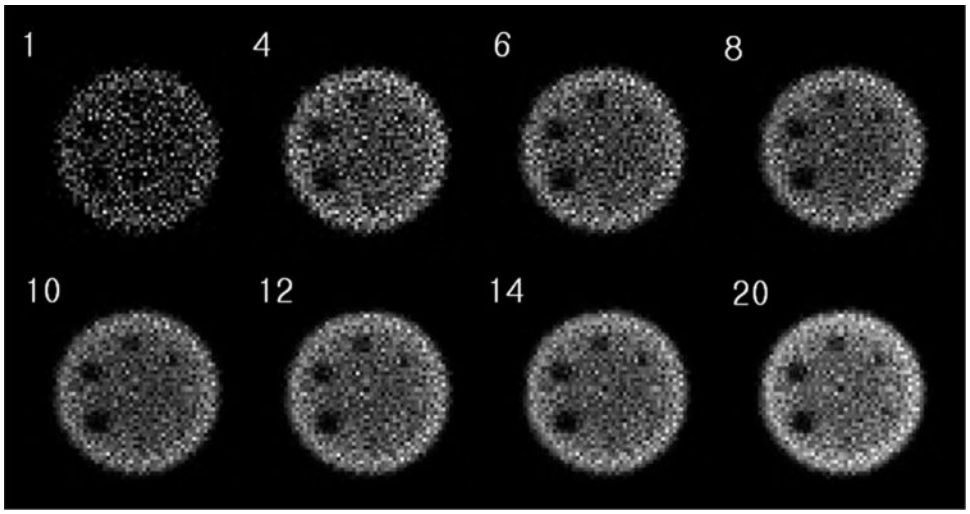

Figure 5.

Accumulated images. Summation of low-count images reconstructed from each sub-sinogram. The numbers at the top of the images represent the number of summed low-count images. The noise indices for these images were 0.9561, 0.4901, 0.4239, 0.3684, 0.3231, 0.3142, 0.2912, and 0.2612, respectively. The ROI for the calculation of noise index was the center uniform area. The radius of the ROI was 6, and the number of pixels in the ROI was 112.

Author Manuscript Author Manuscript Author Manuscript Author Manuscript

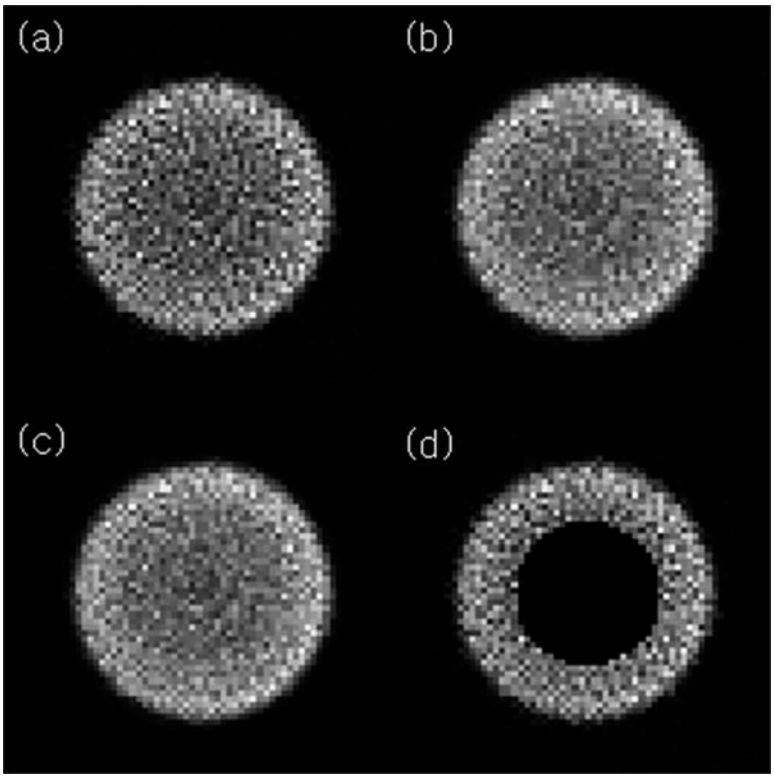

Figure 6.
The reconstructed images. Three reconstructed images using (a) the conventional ML-EM algorithm with a total-sinogram, (b) the ML-EM with 20 sub-sinograms, and (c) the ML-EM with 1000 combinations of sub-sinograms. Noise indices were calculated over the ROIs (d). Noise indices were 0.3218, 0.2313, and 0.2175 for (a–c), respectively.

Author Manuscript Author Manuscript Author Manuscript Author Manuscript

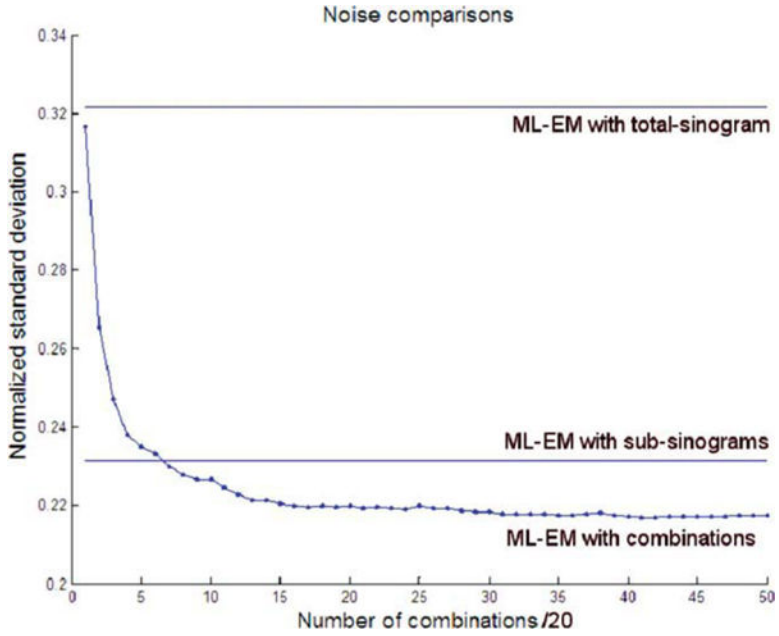

Figure 7.

Noise indices. The noise index is the standard deviation divided by its mean over a uniform area. The upper and lower horizontal lines represent the noise indices of the ML-EM using the total-sinogram and the ML-EM using 20 sub-sinograms, respectively. The curve is the noise index of the ML-EM using combinations of sub-sinograms as a function of the number of combinations. [Color figure can be viewed in the online issue, which is available at wileyonlinelibrary.com.]

Author Manuscript Author Manuscript Author Manuscript Author Manuscript

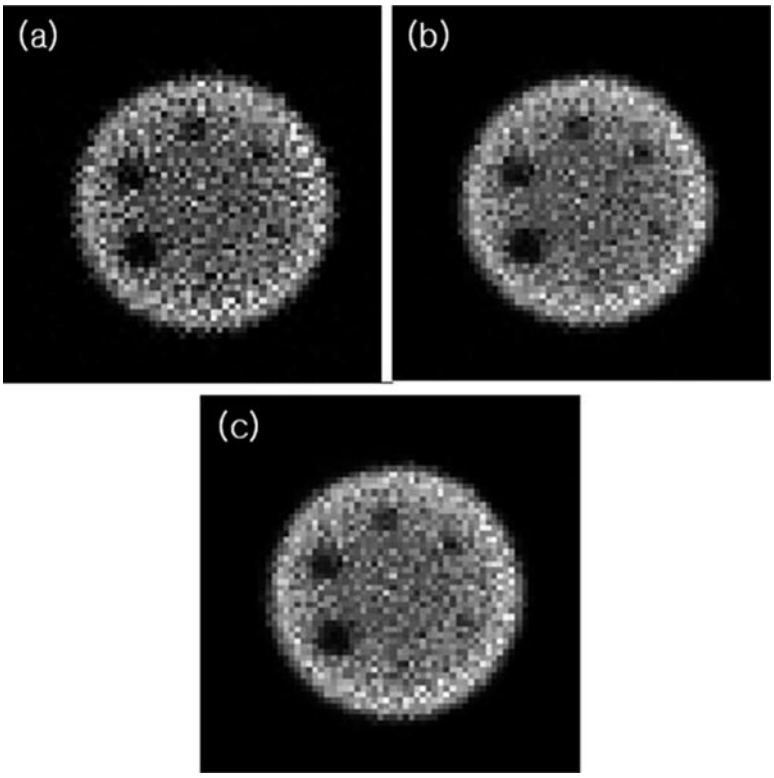

Figure 8.
Reconstructed images of (a) the conventional ML-EM with the total-sinogram, (b) ML-EM with 20 sub-sinograms, and (c) ML-EM with 1000 combinations of the sub-sinograms. Noise indices over the central uniform area were 0.3459, 0.2612, and 0.2362, respectively. The radius of the ROI was 6. The number of pixels in the ROI was 112.

Author Manuscript Author Manuscript Author Manuscript Author Manuscript

Table I

Noise indices from the postfiltered images with 2D Gaussian convolution kernels.

σ	Method	ROI 1	ROI 2	ROI 3	ROI 4	Mean
0.5	Total[a]	0.1928	0.1128	0.1974	0.1170	0.1550
	Sub[b]	0.1643	0.1023	0.1741	0.1152	0.1390
	Comb[c]	0.1627	0.1037	0.1642	0.1106	0.1353
0.7	Total	0.1111	0.0565	0.1101	0.0621	0.0850
	Sub	0.0986	0.0525	0.1000	0.0620	0.0783
	Comb	0.0981	0.0529	0.0955	0.0608	0.0768
1.0	Total	0.0852	0.0382	0.0811	0.0453	0.0625
	Sub	0.0780	0.0363	0.0746	0.0455	0.0586
	Comb	0.0770	0.0360	0.0723	0.0451	0.0576

[a]Total: total-sinogram method.

[b]Sub: sub-sinogram method.

[c]Comb: combination method.